Journal of Minerals & Materials Characterization & Engineering, Vol. 8, No.6, pp 439-453, 2009
jmmce.org

Nucleation Reduction Strategy of $SrNH_4MgHPO_4$ (Strontium Ammonium Magnesium Hydrogen Phosphate) Crystal Growth in Silica Gel Medium and Its Characterization Studies

J. Kishore Kumar[1], R. Ramesh[1], G. Kanchana[2], P. Suresh[1] and P. Sundaramoorthi[1*]

[1]*Department of Physics, Thiruvalluvar Govt. Arts College, Rasipuram, Namakkal, India-637401*
[2]*Department of Biochemistry, Muthayammal College of Arts and Science, Rasipuram, Namakkal, India-637408*

**Corresponding Author: E-mail: moorthi.sundara@gmail.com, Ph-04287-252785, Cell-9486902430*

Abstract

Kidney stones consist of various chemical compounds. Mineral oxalate monohydrate and di-hydrate is the main inorganic constituent of kidney stones. However, the mechanisms for the formation of crystal mineral oxalate are not clear. In this field of study, there are many theories including nucleation, crystal growth and or aggregation of formation of crystals .The effect of some urinary species such as ammonium oxalates, calcium, citrate, proteins and trace mineral elements have been previously reported by the author. The kidney stone constituents are grown in the kidney environments, the sodium meta silica gel medium (SMS) provides the necessary growth simulation (in-vitro). In the artificial urinary stone growth process, growth parameters within the different chemical environments are identified. The author has reported the growth of urinary crystals such as CHP, SHP, BHP and AHP. In the present study, $SrNH_4MgHPO_4$ (Strontium Ammonium Magnesium Hydrogen Phosphate) crystals have been grown in three different growth faces to attain the total nucleation reductions. As an extension of this research, many characterization studies have been carried out such as FTIR, XRD, TGA/DTA, SEM and etching and the results are reported.

Key words: *Trace element, Strontium, MHP, AHP, SMS gel and renal stone.*

1. INTRODUCTION

All kidney stones consist of a complex matrix with bio-minerals. The organic matrix has a composition that remains constant regardless of the type of crystals that make up the stone [1, 2]. The urinary stone matrix accounts for approximately 3% of weight of a calculus [3]. From the analysis, the matrix compounds are soluble [4]. The most recent knowledge of the matrix has been described as a heterogeneous material composed of organic, inorganic and semi organic compounds like protein, lipids, carbohydrates and cellular minerals etc. [5]. Proteins are the major constituents of stone matrices and the principle macromolecule in the urine [6]. Urinary proteins with the potential to adjust crystallization of mineral oxalates and calcium phosphate are Tamm-Horsfall protein, nepheromineralin, osteopontin, calprotectin, human serum albumin and urinary prothrombin fragment [5]. The kidney, chiefly by the renal tubular epithelial cells, produces most of the proteins. Other protein such as calprotectin, which is produced by granulocytes are commonly released at the sites of inflammation, has also been of concern in stone formation. The bio-minerals contain hard minerals like Ca, Ba, Sr, Mg and phosphates or its mixtures. The most common and important human body element of all the stones is calcium. Naturally calcium is found at concentrations of 8.9-10.1 mg/ml in the plasma [7]. Hypermineraluria is a biological syndrome defined as excretion in the urine of more than 0.1 mmol / kg / 24 hours of major minerals. Hypermineraluria is the most common metabolic abnormality in patients with nephrolithiasis [8].

Hypermineraluria raises urine supersaturation with respect to the solid phase of mineral complex with phosphate, enhancing the probability of self-nucleation and growth in to clinically significant stones. Urinary mineral excretion is continuously influenced by dietary intakes of calcium, sodium, protein, carbohydrates, alcohol, ammonium, trace element and potassium [9]. A mineral has been shown to bind to oxalate to form mineral oxalate monohydrate. Thus, mineral has been shown to affect the concentration of oxalate. In addition, oxalate is a major component of urinary stones and its urinary concentration plays an important role in stone formation. Even a small increase in urinary oxalate has a significant impact on mineral oxalate saturation. Although primary hyperoxaluria is relatively uncommon, patients with mineral oxalate stones have some degree of hyperoxaluria [10]. More amounts of oxalate can be obtained from foods such as nuts, chocolate, and dark green leafy vegetables [11]. A citrate concentration of plasma ranges from 0.05-0.03 mmol / liter and it exits as an alkaline citrate [12]. Citrate inhibits crystallization of mineral oxalate and mineral phosphate by several mechanisms. (a) It decreases urinary saturation of mineral salts by complexion minerals and reducing ionic minerals concentration [13]. (b) Citrate directly inhibits spontaneous precipitation of mineral oxalate [14], agglomeration of mineral oxalate [15], crystal growth of mineral phosphate [13] and heterogeneous nucleation of mineral oxalate by monosodium urate [16]. (c) Citrate converts glycoproteins to an active disaggregated state probably by enhancing their inhibitor activity against the crystallization of calcium salts [17-18]. Due to the inhibitory role of citrate mentioned above, patients with hypocitraturia would be at a higher risk of minerals containing renal stones.

The kinetic process of AOMH (Ammonium Oxalate Monohydrate) nucleation and crystal growth requires super saturation [19], which can be obtained by excretion of the reactants in the urine (ammonium ion, calcium, trace elemental oxalate and water). A few molecules are combined together to form clusters. In the early step, clusters do not show a high degree of internal ordering. The longer time they exist, however, their degree of ordering increases by replacing internal salvation bonds by solid ion-ion bonds. Gradually, clusters become crystal embryos [20-21]. Above a critical size, embryos will grow into stable nuclei, and below some critical size, crystal embryos are too small and will reduce over all free energy by dissolving. The size of the nuclei is usually 100A° or less [21]. Once a crystal nucleus has reached its critical size and super saturation ratio remains above one, the overall free energy is decreased by adding new crystal components to the nucleolus (self/spontaneous growth). This process is technically referred to as crystal growth.

2. MATERIALS AND METHODS

The silica gel also known as water glass was used in the present work as an intermediate growth medium. SMS (ARG-sodium meta silicate powder) was added to the double distilled water, in the ratio of 1:1, mixed, stirred well and kept undisturbed for few days to allow sedimentation. Then the clear top solution was filtered and stored in a light protected glass container. This is known as a stock solution [22]. Gel densities of 1.03-1.06 gm/cc were used. Simple test tubes of 25 mm diameter and 150 mm length were used as growth apparatus. The concentration of orthophosphoric acid used in this experiment was 0.5N, 1N and 2N. The concentration of supernatant solution [$SrCl_2$+NH_4Cl_2+$MgCl_2$] varied from 0.5:0.5:0.5 M to 2:2:2 M [23-24]. One of the reactants orthophosphoric acid was mixed within the gel solution. The gel solution was taken as one third of its volume of the test tubes and after the gel set, the supernatant solution was added slowly along the sides of the test tubes. The mixture diffuses through the gel medium, which contains orthophorphoric acid and the self nucleation starts which in turn leads to the growth of $SrNH_4MgHPO_4$ crystal.

The chemical reaction is

$$Sr^{2+}+NH4^{2+}+Mg^{2+}+HPO_4^{2-}+2H_2O \Rightarrow SrNH_4MgHPO_4.\ 2H_2O + Waste$$

The crystal growth processes were carried out in three different environments, one within laboratory environment, second one was sunlight exposed environment (day time only-7 hours per day) and another one was continuous (with suitable SMPS arrangement) semiconductor laser light exposed environment.

Table -1 Growth parameters of $SrNH_4MgHPO_4$ crystals (SDP)

SMS gel density gm /cc	Ortho phosphoric acid concentration in N	Gel+ H_3PO_4 pH value	Gel setting time in hrs	Supernatant solution concentration [Strontium chloride + Ammonium chloride + $Mg(NO_3)_2 . 2H_2O$] in M	Nucleation observed in hours	Growth period in days	Types of crystal observed
1.03	1	6.4	24	**1:0.5:1**	26	**270**	**Many poly crystals**
		6.9	**18**	**-Do-**	**29**		
		7.2	34	-Do-	90		
	1.5	6.5	14	**1:1:1**	20	**280**	
		7.0	**11**	**-Do-**	**70**		**Liesegang rings are observed**
		7.9	28	-Do-	84		
1.04	1	**6.4**	**39**	**1:1:1**	**80**	**279**	
		6.9	**16**	**-Do-**	**74**		
		7.2	48	-Do-	68		
	2	6.7	19	**0.5:1:1**	23	**265**	**Single crystals**
		6.8	**15**	**-Do-**	**44**		
		7.6	24	-Do-	74		

N- Normality, M- Molarity

3. RESULTS AND DISCUSSION

The $SrNH_4MgHPO_4$ crystals are grown in three different growth faces by applying various growth parameters. Figures 1-3 shows the growth of $SrNH_4MgHPO_4$ crystals at different growth environments and Figure-4 shows the harvested $SrNH_4MgHPO_4$ crystal. Table-1 gives the growth parameters of $SrNH_4MgHPO_4$ crystals and the bold letters represents the optimum growth parameters. Among them, the laser exposed (4 mW, 7800Å of continues semiconductor laser light power and wave length are used) growth medium shows better nucleation reduction and no crystals were formed, because of the inability to attain super saturation. In sun light exposed medium partial nucleation was observed, since exposure of sunlight to the growth medium was only in the day time, that is seven hours per day and the growth period was six months.

Fig.1 Growth of $SrNH_4MgHPO_4$ crystals within the laboratory environment

Fig. 2 Growth of $SrNH_4MgHPO_4$ crystals within sunlight exposed medium

Fig. 3 Growth of $SrNH_4MgHPO_4$ crystals in laser light exposed medium

Fig. 4 Harvested $SrNH_4MgHPO_4$ crystal

3.1. FTIR Spectral Analysis of $SrNH_4MgHPO_4$ Crystals

$SrNH_4MgHPO_4$-FTIR spectrum was recorded by using SHIMADZU FTIR-435 instrument. The FTIR spectrometer has KBr pellets sample holder and a KBr detector. The KBr pellet samples were used and the absorption frequencies start in the range from 400 cm^{-1} to 4000 cm^{-1}. The spectrum was interpreted with the earlier reported values [25-27]. The absorption bonds, absorption frequencies and percentage of transmittance are tabulated in Table-2.

Table-2 Comparative study of the FTIR-Spectrum of $SrNH_4MgHPO_4$ crystal

S.No.	Bonds/vibrations	Reported values cm^{-1}	Observed values cm^{-1}	% of absorption value
01.	Sr, NH-asymmetric stretching mode& Hydrogen bond	3284	3271.69	1.165
02.	H-O-H Symmetric stretching bond	1651	1658.70	0.670
03.	NH in plane stretching	1238.2	1237.71	0.680
04.	P=O bonding stretching bond	1217-1137	1166.35	0.861
05.	PO_4 bond	1000 - 1100	1117.12	1.361
06.	PO_4-asymmetric stretching mode	874	895.34	0.747
07.	Acid phosphate	577	565.27	0.810

3.2. Thermo Gravimetric (TGA and DTA) Analysis of $SrNH_4MgHPO_4$ Crystals

The TGA and DTA of $SrNH_4MgHPO_4$ crystals were carried out by STA 11500-PLTS instruments. The $SrNH_4MgHPO_4$ crystal, a 5.976 mg sample, was used for the TGA process. The TGA was ramped from room temperature to 900^0C by heating at a constant rate. The percentages of weight loss of the $SrNH_4MgHPO_4$ sample at a particular temperature are tabulated in Table-3.

The expected thermo-chemical reactions are

$$SrNH_4MgHPO_4.2H_2O \xrightarrow{\Delta} SrMgHPO_4 + NH_3\uparrow + 2H_2O\uparrow$$

$$2SrMgHPO_4 \xrightarrow{\Delta} 2Sr\,Mg + (PO_4.H_2O)\uparrow + \frac{3}{2}O_2\uparrow \text{ up to } 900^{\circ}C$$

Beyond 100ºC, the sample becomes anhydrous and after that it is hydrous along with ammonia up to 365ºC and 59% of the sample remained stable at the end of the analysis. Sr and Mg (Strontium and Magnesium) are stable up to 950 ºC.

Table-3 TGA and DTA of $SrNH_4MgHPO_4$ crystal

Points	TGA			DTA in ^0C
	Temperature (ºC)	% of $SrNH_4MgHPO_4$ crystal present	Quantity of sample remaining in milligrams	
1	30	100	5.976	-
2	77.20	99.563	5.949	75.37
3	133.22	75.084	4.487	126.03
4	188.72	64.122	3.832	162.22
5	364.79	59.447	3.552	225.04
6	364.79	59.447	3.552	346.78
7	364.79	59.447	3.552	685.13
8	560	59	3.526	706.31
9	950	59	3.526	-

3.3. Etching Studies of $SrNH_4MgHPO_4$ Crystal

A well-grown $SrNH_4MgHPO_4$ crystal was immersed in HCl solution at a desired concentration. The dissolution of the $SrNH_4MgHPO_4$ crystal depends on the etchant concentration, temperature, crystal morphology, etching time etc. Fig-5 shows the etch pits of $SrNH_4MgHPO_4$ crystal [28-31]. The etch pit patterns are observed as spirals, dendrites, vallies of ups, downs and straights.

Fig. 5. Etch pit pattern of $SrNH_4MgHPO_4$ crystal.

3.4. Scanning Electron Microscopic Studies of $SrNH_4MgHPO_4$ Crystal

A well-grown $SrNH_4MgHPO_4$ single crystal was selected for the investigation of surface morphology of the grown crystal by using SEM. The SEM photograph was obtained in a version S-300-I instrument. The sample named as VCA-600 was kept in lobe middle; the data size was 640 x 480 µm. The difference between the minor and major magnification of SEM was about 500 times. SEM acceleration voltage was 25000 volts and the sample was kept in high vacuum state. A 18200- µm work distance was maintained and monochromatic color modes were employed. Fig-6 shows the SEM pattern of the $SrNH_4MgHPO_4$ crystal of 200 µm magnification [32-35].

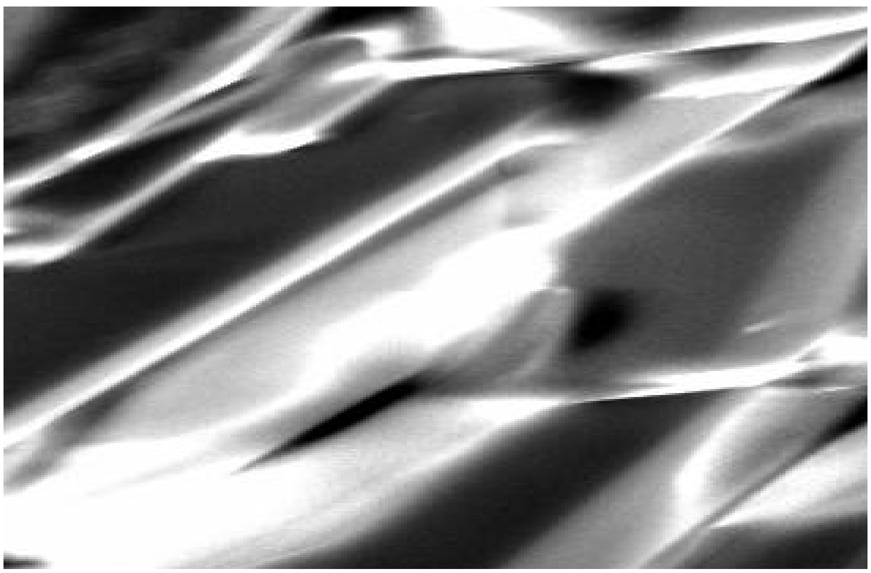

Fig. 6 SEM photo of $SrNH_4MgHPO_4$ crystal

3.5. X-ray Diffraction

The XRD results revealed that the grown crystal was in single phase of $SrNH_4MgHPO_4$. The XRD pattern and diffraction indices of the grown crystals are calculated. Using the treor program crystal cell parameters are calculated. The unit cell parameters of $SrNH_4MgHPO_4$ crystals are a =18.06 Å, b=18.57 Å, c=22.72 Å and $\alpha=\beta=\gamma=90^{o}$. The crystal system is identified as **orthorhombic**. The volume of the $SrNH_4MgHPO_4$ unit cell is 7619.702 $(Å)^3$.

4. CONCLUSION

The $SrNH_4MgHPO_4$ (Strontium Ammonium Magnesium Hydrogen Phosphate) crystals were grown at room temperature, and exposed to sunlight and laser medium. It was found that the $SrNH_4MgHPO_4$ crystal nucleation rate has been reduced more in the laser exposed medium than the sunlight-exposed medium, which is due to a variation of super saturations. The FTIR-spectrum recorded the functional group frequencies of $SrNH_4MgHPO_4$ crystal constituents. These results are recorded and compared with the reported values. Chemical etchings have been done at room temperature, which revealed the grown crystal defects. SEM analyses were also done and it reveals the surface morphology of $SrNH_4MgHPO_4$ crystal. The decomposition temperature and percentage of weight loss of the grown crystal are recorded by TGA and DTA analysis. XRPD data provides the $SrNH_4MgHPO_4$ grown crystal cell parameters and its structure. This investigation results can be discussed with nephrologists and the results can be applied to the human physiological system in stepwise manner to avoid the renal stone formation. The crystal can be further investigated by atomic forced microscopy (AFM) to study the atomic orientation of renal stones with in the human physiological system.

REFERENCES

[1] S.R.Khan, P.O.Whalen and P.A.Glenton, J.Cryst.Growth 134 (1993) 211.
[2] W.H.Boyce, Am.J.Med.45 (5) (1968) 673.
[3] H.G.Tiselius, Clin.Chim.Acta.122 (1982) 409.
[4] R.W.Marshall and W.G.Robertson, Clin.Chim.Acta.72 (1976) 253.
[5] S.R.Khan, Urol.Int 59 (1997) 59.
[6] R.L.Ryall, A.M.F.Stapleton, in calcium oxalate in Biological system, Edi.S.R.Khan (CRC press) (1995).
[7] C.G.Duarte and F.G.Knox, in text book of renal pathophysiology (Harper and Row (1978).
[8] F.L.Coe, J.H.Parks and J.R.Asplin, N.Engl.J.Med. 327 (1992) 1141.
[9] Maurice Audran and Erick Legrand, Joint Bone spine 67(6) (2000) 509.
[10] Y.Ogawa, T.miyazato and T.Hataano,World j.Surgery, 24(10) (2000) 1154.
[11] D.S.Goldfarb and F.L.Coe, Am.Fam.Physicican,.60(8) (2000) 2269.
[12] D.P.Simpson, Am.J.Physiol.,.224(3)F (1983) 223.
[13] J.L.Mayer and L.Hsmith, Invest.Urol., 13 (1975) 36.
[14] M.J.Nicar, K.Hill and C.Y.C.Pack, J.Bone. Miner.Res., 2 (3) (1987) 215.
[15] D.J.Kok, S.E.Papapoulus and O.L.M.Bijvoet,Lancet, 41 (1986) 1056.
[16] C.Y.C. Pak and Paterson, Arch.Intern.Med.146 (1986) 863.
[17] B.Hess, Miner.Electr.Metab., 20 (1996) 393.
[18] C.Y.C.Pak, Hypocitraturia; a critical review and furture direction,from 8th European symposium on Urolithiasis-Parma,Italy,June 9-12 (1999).
[19] A.Mersmann,Crystallization technology,Hand book,2nd Edi. Marcel Dekker,Inc., (2000).
[20] V.A.Garten and R.B.Head,Phil.Mag.,14 (1966) 1243.
[21] D.J.Kok, The role of crystallization process in mineral oxlates urolithasis, Ph.D thesis,Univerasity of Leiden. (1991).
[22] H.K. Henisch, J Electro Chemical. Soc., 112 (1965) 627.

[23] A.E.Alexander and P.Honson, Colloid Science, Clarendon Press, Oxford, (1949).
[24] W.Eitel, In:Physical chemistry of Silicate University of Chicago Press (1954).
[25] Yean. Chin, J. Urol.,. Vol 86, (1961) 838-854.
[26] C.M. Corns, Ann. Clin. Bio-Cherm, Vol 20, (1983) 20-35.
[27] A.Hesse , D. Bach,. Stone analysis by IR spectroscopy, Clinical and laboratory Aspects, Edi.Alan Rose, University Park Press, Baltimore, PP.87-105, 1982.
[28] J.J.Gilman, J.Johnsion and G.W.Sears, J.Appl.Physics, 29 (1958) 749.
[29] J.J. Gilman, J.Appl.Physics, 27 (1956) 1018.
[30] J.C.Fisher, in: Dissolutions and Mechanical Properties of Crystals, John Wiley and sons, NewYork (1957).
[31] J.B. New Kirk, in: Director observation of Imperfection in crystals, Inter science Publisers, New York (1962).
[32] K. Taukamot, J. Cryst. Growth, 61 b (1983) 99.
[33] H.C.Gates, Thirty years of progress in Surface Science, in: Crystal growth and characterization,(Edi),North Holland, 1975.
[34] H.Bethage, et al, Electron Microscopy in Solid State Physics, Elsevier, Amsterdom, 1987
[35] N. Albon et al, in: Growth and Perfection of Crystals, Wiley, New York, 44, 1958.